

The effect of pick orientation on rock fragmentation

Seyed Saleh Mostafavi, Qingyu Yao & L.C. Zhang

School of Mechanical and Manufacturing Engineering, The University of New South Wales, NSW, Australia

Jason Lunn & Craig Melmeth

Bradken, Mayfield West, NSW, Australia

ABSTRACT: Efficient rock breakage in terms of energy consumption and dust generation is significantly important. This research investigates the effect of pick orientation on the efficiency of breaking rocks in terms of cutting force and energy. The study was carried out by simulating a series of edge chipping tests with a pyramidal indenter. The results were verified by relevant experiments on concrete. Three different orientations were chosen. It was found that the best orientation is when the front face is in parallel with the free surface of a rock specimen. In this case the size of crushed zone and the amount of energy dissipated in forming the crushed zone is the least.

Subject: Modelling and numerical methods

Keywords: mechanical excavation, mining

1 INTRODUCTION

1.1 Rock fragmentation

Efficient rock breakage in terms of energy consumption and dust generation has drawn significant attention. Extensive research has been done to find the optimized geometrical parameters of the cutting picks and to develop more efficient mechanical fragmentation techniques. In order to improve mechanical fragmentation systems, knowledge of the mechanism of crack propagation under a sharp indenter is essential. There are some basic experiments to investigate crack propagation and to assess pick performance, among which the Edge chipping test has been regarded as a good fragmentation process because it is highly efficient to generate fracture (Larson 1987). Rock cutting can be considered as a series of successive cycles of edge chipping, of which each is composed of a crushing and chipping phase. The force/energy information from such experiments can be used for the design and optimization of cutting picks. Figure 1 shows a chip formed in an edge chipping experiment where d_c is the cutting depth which

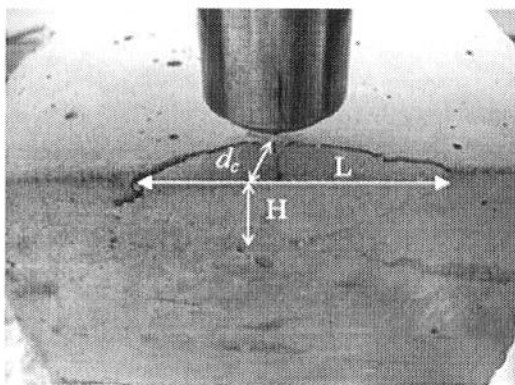


Figure 1. A chipping test and the geometry of a chip.

is the distance from indenter tip to the edge of the specimen, H is the chip height, and L is the chip length.

In this research we will investigate the orientation influence of a pyramid indenter on cutting force and energy consumption. We chose three different orientations of the pyramid indenter in relation to the free surface of a specimen, i.e., (a) one edge perpendicular to the surface, (b) one edge tilted in 22.5 degrees to the surface, and (c) one face of the indenter being parallel to the free surface as shown in Fig. 2. Numerical modeling of the chipping process requires a constitutive model that can describe the material behavior under severe hydrostatic stresses followed by crack initiation and chipping. The analysis will be carried out by the finite element method using a commercially available code, LS-DYNA, along with a constitutive model integrated with a damage model.

1.2 Theory of the constitutive model

The continuous surface cap model (CSCM) in the materials library of LS-DYNA is appropriate for brittle materials like rocks and concrete. It can be used to integrate with damage development to describe deformation and fragmentation in a brittle material. Two types of damages are integrated with the CSCM: (a) the ductile damage which accumulates when the mean stress is compressive and the strain energy exceeds

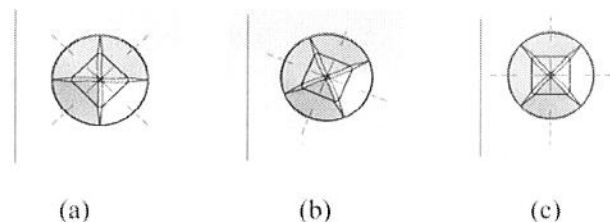


Figure 2. Schematic views of different orientations of pyramid relative to free surface, a) one edge perpendicular to free surface, b) one edge at 22.5 degrees to free surface, c) front face parallel to free surface.

the damage threshold τ_{0c} , and (b) the brittle damage which accumulates when the mean stress is tensile and the strain energy exceeds the damage threshold τ_{0t} . Here, the strain energies of the ductile and brittle damages are defined by:

$$\tau_c = \sqrt{\frac{1}{2} \sigma_{ij} \varepsilon_{ij}} \quad (1)$$

$$\tau_t = \sqrt{K \varepsilon_{ij}^2} \quad (2)$$

The stresses are first obtained without considering the damage. They will then be degraded based on a scalar damage parameter, d , by

$$\bar{\sigma}_{ij} = (1-d)\sigma_{ij} \quad (3)$$

where $\bar{\sigma}_{ij}$ the damaged stress and d is the maximum of the ductile and brittle damage defined by [2]:

$$d(\tau_c) = \frac{0.999}{B} \left[\frac{1+B}{1+B \exp(-A(\tau_c - \tau_{0c}))} - 1 \right] \quad (4)$$

$$d(\tau_t) = \frac{0.999}{D} \left[\frac{1+D}{1+D \exp(-C(\tau_t - \tau_{0t}))} - 1 \right] \quad (5)$$

In Eq. (3), $d=0$ corresponds to the undamaged or uncracked state and $d=1$ defines the complete failure. In Eq. (4) and (5), A , B , C and D , determined by experiment, define the shape of softening in stress-displacement or stress-strain curves. To calibrate the damage model, experimental data from an unconfined compression test are required, of which the details can be found in (Ls-Dyna keyword 2007, Schwer 2003). A sample of concrete with grain size of 10 mm and Uniaxial Compressive Strength of 48 Mpa is used in this model.

2 EXPERIMENTAL SETUP

A specimen used in experiment was a block of concrete of dimensions $150 \times 150 \times 150$ mm. The edge chipping tests were carried out on an INSTRON 5567 machine at the loading speed of 1 mm/min. The depth of cut was 5 mm as shown in Fig. 1.

2.1 Boundary condition and the FE model

The control volume of the FE model was $35 \times 50 \times 35$ mm, consisting of 260,615 constant stress solid elements. To characterize the damage deformation, no symmetric conditions can be used for both the specimen and indenter. In order to prevent zero deformation modes (Hourglassing) in the elements, the Hourglass control card of Type 1 with coefficient of 0.05 was applied. The lower surface of the control volume was constrained in all degrees of freedom but the rest of the surfaces were free. The indenter was moved down vertically at a speed of 1.5 mm/sec. The contact between the indenter and the specimen was modeled by the automatic surface-to-surface contact in LS-DYNA. To avoid any artificial material interpenetration, the contact formulation of Type = Soft 1 and contact thickness of 0.1 mm was used. The coefficient of friction was taken as 0.6.

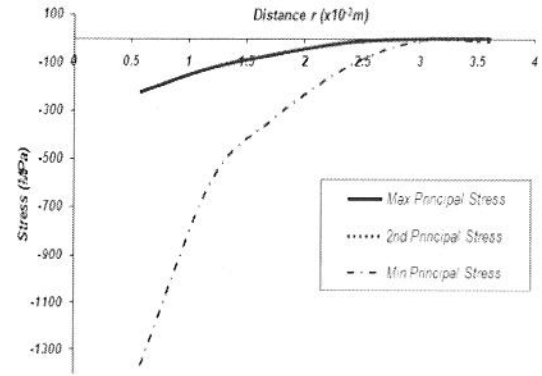


Figure 3. Principal stresses and the radius of crushed zone along the direction of the cracks, for the case (a).

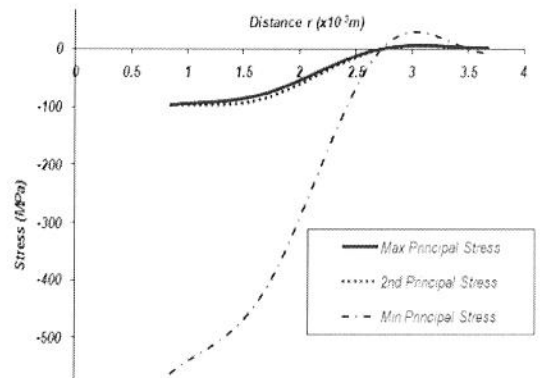


Figure 4. Principal stresses and the radius of crushed zone along the direction of the cracks, for the case (b).

3 RESULTS AND DISCUSSION

Crack initiation and propagation path are determined by the stress distribution due to indentation. The stress state from the simulation shows that a zone with a very high triaxial compressive stresses is present just beneath the indenter. The stress in this zone is always above the compressive yield strength of the material, even more than its brittle/ductile transition stress. Therefore a very large plastic compaction is expected there which in turn causes the rock to be broken or crushed (Van Kesteren 1995). Previous studies (Swain and Lawn 1976; Mishnaevsky 1995; Mostafavi, Zhang et al. 2010; Bao, Zhang et al. 2011) show that about 70 to 85 percent of the external work done by the indenter is dissipated by the formation of the crushed zone. So the size and extent of the crushed zone is a major factor in the efficiency of rock fragmentation. Figures 3 to 5 show the principal stresses and the radius of the crushed zone (r) along the direction of the cracks.

The results indicate that the maximum compressive stress in Orientation (a) of Fig. 2 is the highest compared with those under other orientations. In this case, the radius of the crushed zone along the direction of the cracks is also the largest. It is therefore reasonable to expect that this orientation has the highest energy dissipation to form crushed zone. Fig. 6 compares the external work done by indenters under different orientations, and confirms the above expectation, i.e., Orientation (a) consumes the highest energy.

As the indentation proceeds the boundary of the crushed zone extends to the surrounding elastic region until the

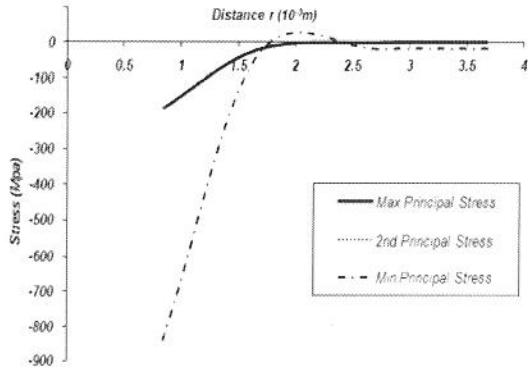


Figure 5. Principal stresses and the radius of crushed zone along the direction of the cracks, for the case (c).

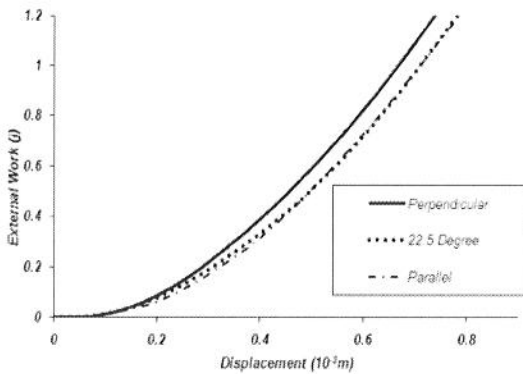


Figure 6. The external work done by the indenter with different orientation.

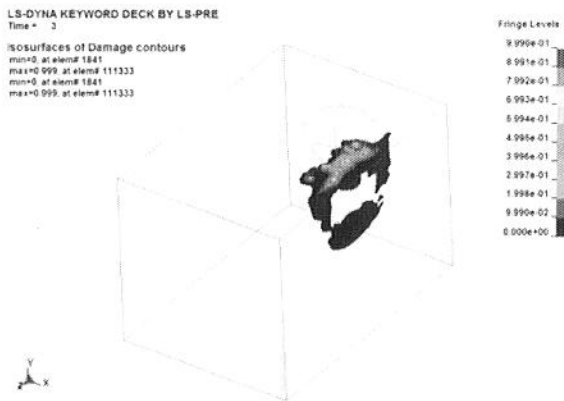


Figure 7. Development of a penny-shape crack and deviation of the parallel cracks toward the free surface of the specimen at the indentation time of 3 second (Orientation b).

maximum tensile stress in the region reaches the crack initiation threshold. Figure 7 and 8 show development and propagation of damage during edge chipping and the top view of the damage zone for the orientation (c). The results demonstrate that radian-median cracks form in parallel to the free surface and propagate downward and parallel to the front surface to form half penny crack. After a certain length, the crack tips from both sides on the surface deviate toward the free edge and finally intersect, leading to chipping.

It can be seen that the cracks initiate along the diagonal of the pyramid, so for the case that diagonal is tilted toward the free surface, propagation of the crack toward the edge

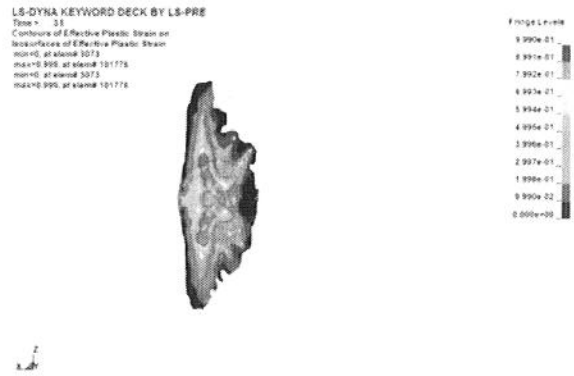


Figure 8. Top view of the damage zone under the indenter with Orientation (c), the crack is formed along the diagonal tilted toward the free surface of the specimen (indentation time at 3.5 second).

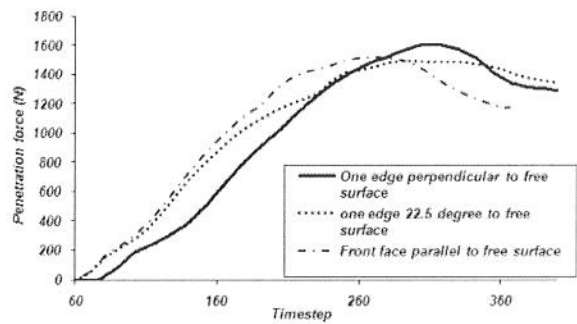


Figure 9. Simulation results of the penetration force for different orientations.

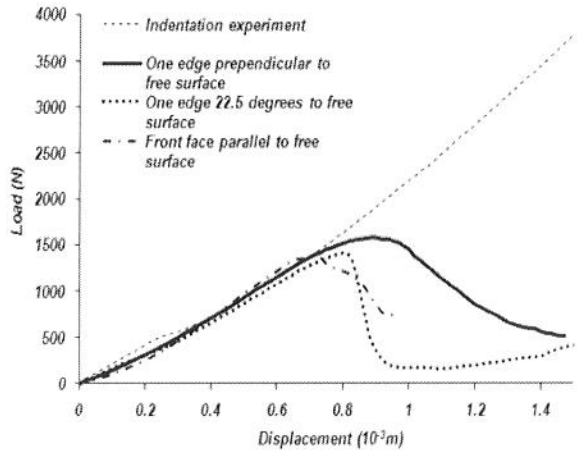


Figure 10. Experiment results of the penetration force in edge chipping with different orientations in compare with indentation test.

and formation of chips needs lower indentation force. So both chipping force and external work done by indenter would be lower for Orientations (b) and (c) where diagonals are tilted toward free surface. For Orientation (b) where one edge of the diagonal is closer to surface, damage is not symmetric and more concentrated under the edge which is closer to free surface. Figure 9 shows the variation of maximum chipping force for the three different orientations, where (c) has the minimum cutting force but the difference is not remarkable. The load displacement curves from the experiments on concrete (Fig. 10) also show that chipping load for Orientations (a) and (c) are

the highest and lowest, respectively, but the difference is not remarkable.

4 CONCLUSION

The orientation of cutting picks in the holder is important in terms of energy efficiency of the cutting. The radius of the crushed zone along the direction of the cracks and the maximum compressive stress in the crushed zone for Orientation (a) where an edge of the pyramid indenter is perpendicular to the free surface of a specimen is the highest compared with those other indenter orientations. Therefore this orientation has the worst energy efficiency. The best orientation is when a face of the indenter is in parallel to the sample free surface, i.e., Orientation (c) of Fig. 2.

ACKNOWLEDGEMENT

The work has been supported by the Australian Research Council and BRADKEN®.

REFERENCES

LS-Dyna Keyword Manual, Version 971. (2007). LSTC. CA.

- Bao, R. H., L. C. Zhang, et al. (2011). "Estimating the Peak Indentation Force of the Edge Chipping of Rocks Using Single Point-Attack Pick." *Rock Mechanics and Rock Engineering*
- Larson, D. A., Morrell, R.J and Mades, (1987). An investigation of crack propagation with a wedge indenter to improve rock fragmentation efficiency, *U.S. Bur. Mines Rep. Invest.*
- M. Swain, B. L. (1976). "Indentation Fracture in Brittle Rocks and Glasses." *Int. J. Rock Mech. Min. Sci. & Geomech.* 13: 311–319.
- Mishnaevsky, L. (1995). "Physical Mechanics of Hard Rock Fragmentation under Mechanical Loading: A Review." *Int. J. Rock Mech. Min. Sci. & Geomech.* 32(8): 763–766.
- Mostafavi, S. S., R. H. Bao, et al. (2011). "An Analytical approach to the optimal design of rock cutting tools." *ASCE Journal of Engineering Mechanics*, **Submitted**.
- Mostafavi, S. S., L. C. Zhang, et al. (2010). "Chipping Brittle Materials: A Finite Element Analysis." *Key Engineering Materials* 443: 433–438.
- Schwer, L. (2003). "A Demonstration For Continuous surface Cap Model with Damage Calibration, SE&CS."
- Swain, M. V. and B. R. Lawn (1976). "Indentation fracture in brittle rocks and glasses." *International Journal of Rock Mechanics and Mining Sciences & Geomechanics Abstracts* 13(11): 311–319.
- Van Kesteren, W. G. M., 1995. In: Baler, G., (1995). Numerical simulations of crack bifurcation in the chip forming cutting process in rock. *Fracture of brittle, disordered materials*.